

GRB and Transient Sciences

Yuji Urata¹, Kuiyun Huang²

¹*Institute of Astronomy, National Central University, Chung-Li 32054, Taiwan*

²*Center for General Education, Chung Yuan Christian University, Taoyuan 32023, Taiwan*
urata@g.ncu.edu.tw

Abstract

We overview the science cases of Gamma-ray Burst and transients for the Next Generation Very Large Array (ngVLA). Based on ongoing SMA, ALMA and multi-wavelength observations, there are five science cases; (1) Energetics and acceleration efficiency of GRB and related transients, (2) probe of first-generation stars, (3) GRB-SN-SNR connection, (4) unification of short GRBs as gravitational wave source, (5) relativistic transients as multi-messenger astronomy.

Key words: gamma-ray burst: individual — Submillimeter: galaxies — X-rays: bursts

1. Introduction

Gamma-ray Bursts (GRBs) are among the most powerful explosions in the universe and are observationally characterized according to intense short flashes mainly occurring in the high-energy band (so-called prompt emission) and long-lived afterglows seen from the X-ray bands to radio bands. GRBs are emitted in extremely relativistic jets with Lorentz factor larger than ~ 100 emanating from newly born black holes or magnetars, making it an ideal showcase of relativistic astrophysics (e.g., Mészáros & Rees 1997). Thanks to their exceptional brightness they are visible up to very high redshifts, providing a unique window on the early Universe and the formation of the primordial stars (e.g., Tanvir et al. 2009; Bloom et al. 2009). The majority of long GRBs are believed to be produced at the deaths of massive stars. It is therefore expected that GRBs existed at redshifts where no luminous AGN or galaxies had been formed yet. Long GRBs are excellent probes for the era of the “first star” formation and cosmic re-ionization. On the other hand, Short-GRB have long been suspected on theoretical grounds to arise from compact object binary mergers (NS-NS or NS-BH). The unprecedented observation of short-GRB (GRB170817) coincident with the detection of gravitational wave (GW170817) from coalescing binary NSs in an elliptical galaxy presents the long-awaited smoking gun that binary NS mergers give rise to short-GRB170817 (Abbott et al. 2017). Furthermore GRBs is one of the EM counterpart of neutrino events (Murase & Ioka 2013). Therefore, GRBs have been playing one of the central roles of the multi-messenger astronomy.

2. GRB afterglows and advantages of millimeter/submillimeter observations

Characterizations of the radiation are the most fundamental observational approach for the GRB/transient studies. Observations in radio bands are critical for characterizing the radiations from GRB afterglows and related transient phenomenon. GRBs are believed to result from the conversion of the kinetic energy of ultra-relativistic particles or possibly

the electromagnetic energy of a Poynting flux to radiation in an optically thin region. In this case, the model accepts various central engines (e.g. massive star explosion for long GRBs, and mergers for short GRBs (Figure 1). This generic “fireball” model (Mészáros & Rees 1997) has also been confirmed by the afterglow observations. Therefore, it is reasonable to expect that afterglows can be described by synchrotron emission from a decelerating relativistic shell that collides with an external medium (external synchrotron shock model; Figure 1 & 2).

Based on the external synchrotron shock model, both the spectrum and the light curve consist of several power-law segments with related indices (e.g., Sari et al. 1998). The broad-band spectrum is characterized by the synchrotron peak frequency ν_m and the peak spectrum flux density $F_{v,max}$ as shown in Figure 2. These two parameters are key to the model. The peak frequency is expected to fall at lower frequencies (X-ray to radio) over time (minutes to several days) as $\nu_m \propto t^{-3/2}$. The peak spectra flux density $F_{v,max}$ is predicted to remain constant in the circumburst model, while decrease as $F_{v,max} \propto t^{-1/2}$ in the wind model. Expected critical differences between short and long GRBs are (1) explosion energy scale (short events could be much smaller e.g. $E \sim 10^{51-52}$ erg), (2) circumburst density (events must be thin density condition e.g. $n < 0.1$ cm). Since characterizing frequency and peak flux are fully dependent on these two physical parameters, constraining on $F_{v,max}$ and ν_m using temporal and spectrum observations are crucial. As shown in Figure 2, the radio bands (e.g. ngVLA, ALMA) are critical for characterizing the flux peak and its temporal evolutions.

Based on the external synchrotron shock modeling for actual afterglow observing data, physical parameters can be estimated (explosion energy E , circumburst number density n , observing angle θ_{jet} , synchrotron slope p , magnetic field energy fraction ϵ_B , and accelerated particle energy density fraction ϵ_E). Table 1 is the summary for several examples based on multi-frequency observations (van Eerten et al. 2012; Cenko et al. 2013; Urata et al. 2014; Urata et al. 2015b; Huang et al. 2017). Note that these parameter estimations were performed by assuming 100% of electrons are accelerated at the shocks.

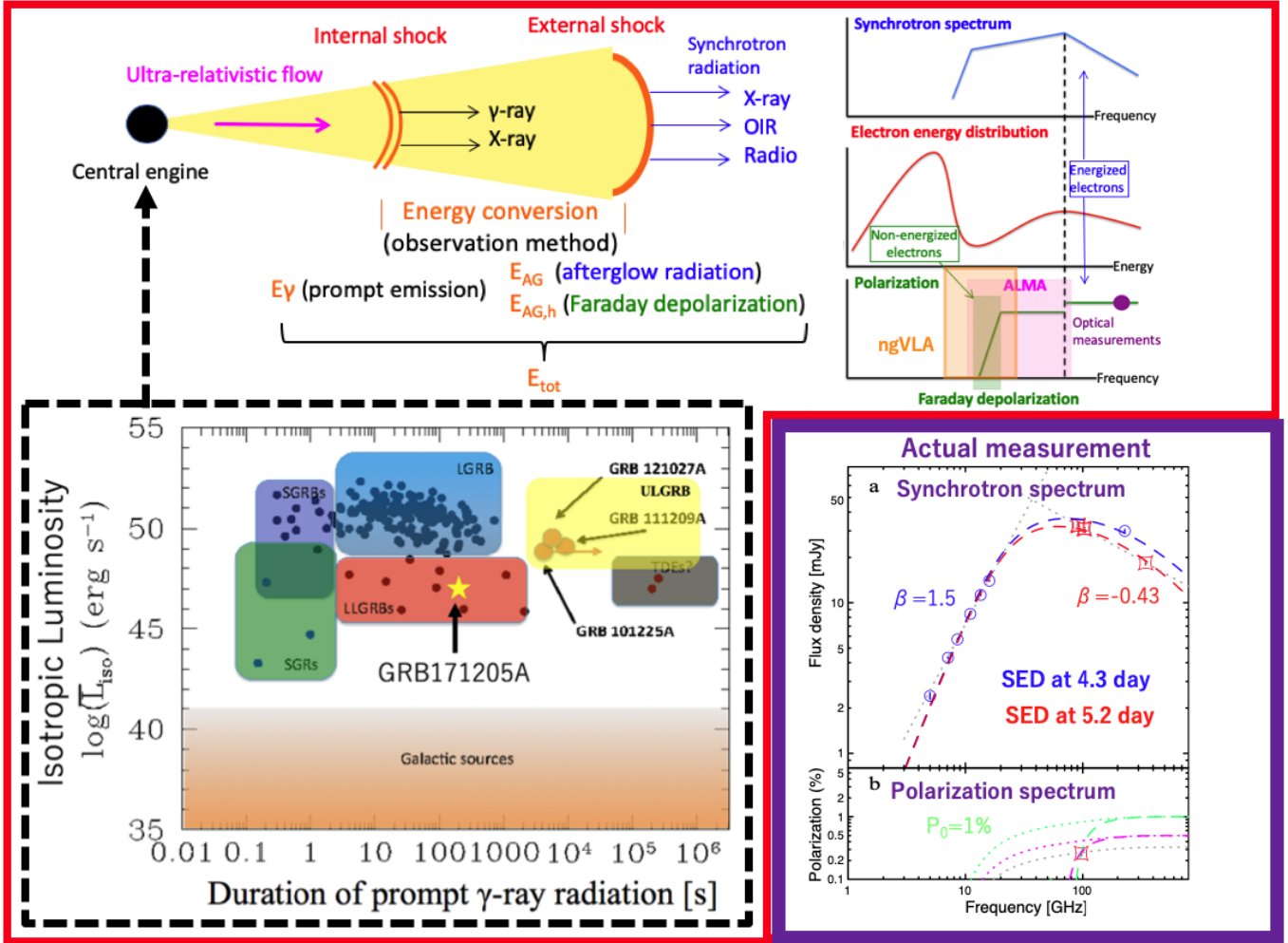


Fig. 1. The concept of GRB energetics (red box). Based on the standard “fireball” model, various central engine (i.e. various kind of GRBs) exist. The total energy of GRB could be estimated by observing prompt and afterglow observations. In the afterglow phase, the fraction of non-energized electrons are critical for estimating the total energy (Toma et al. 2008). Since the non-energized electrons do not emit observable emission, the Faraday depolarization is the key. In the purple box, the first demonstration of the Faraday depolarization is presented (Urata et al. 2019).

Table 1. Summary of burst parameters obtained by observations and numerical modeling

Parameters	020903	080330	990510	131030A	120326A	PTF11agg
Category	XRF	XRF(XRR?)	GRB	GRB	XRR	on-axis orphan(?)
E_{peak}^{src} (keV)	$3.3_{-1.0}^{+1.8}$	< 88	423_{-42}^{+42}	406 ± 22	$107.8_{-15.3}^{+15.3}$	—
E_{iso} (erg)	$1.4_{-0.7}^{+18.0} \times 10^{49}$	$< 2.2 \times 10^{52}$	$2.1_{-0.3}^{+0.3} \times 10^{53}$	$3.0_{-0.2}^{+2.0} \times 10^{53}$	$3.2_{-0.3}^{+0.4} \times 10^{52}$	—
z	0.251	1.51	1.619	1.293	1.798	$0.5 < z < 3.0$
θ_{jet} (rad)	0.10	0.12	0.075	0.15	0.14	0.20
E (erg)	5.9×10^{52}	2.3×10^{52}	1.8×10^{53}	3.4×10^{52}	3.9×10^{52}	9×10^{52}
n (cm ⁻³)	1.1	9.0	0.03	0.3	1.0	0.001
θ_{obs} (rad)	0.21	0.12	0 (fixed)	0 (fixed)	0 (fixed)	0.19
p	2.8	2.1	2.28	2.1	2.5 (fixed)	3.0
ϵ_B	1.4×10^{-3}	1.6×10^{-1}	4.6×10^{-3}	4.4×10^{-2}	1.0×10^{-3}	4×10^{-2}
ϵ_e	2.9×10^{-1}	1.4×10^{-1}	3.7×10^{-1}	2.7×10^{-1}	6.9×10^{-1}	2×10^{-1}
Data	Opt, Radio	Opt	X,Opt,Radio	Opt, ALMA	Opt	Opt, Radio

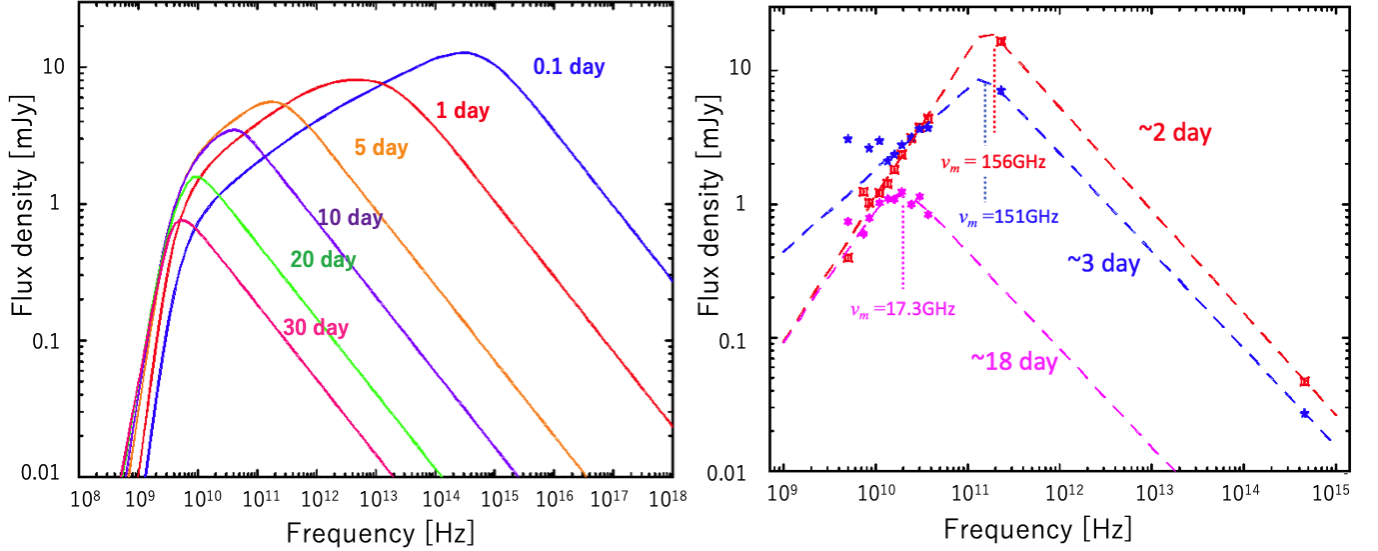


Fig. 2. Temporal evolution of forward shock synchrotron radiation with typical explosion parameters (left). One of example of observed SED evolution using VLA and SMA (right).

Measurements of acceleration fraction are therefore required for estimating actual energetics (§ 3).

3. Energetics and acceleration efficiency

The energetics of GRBs are fundamental physical parameters that cannot only reveal their progenitor systems but also probe both the early and current states of the universe. Although substantial observational efforts have been made since the afterglow discovery, the total energies have been estimated so far without considering non-energized (or non-accelerated), cool electrons at the relativistic collisionless shock (Figure 1) that do not emit observable radiation (Toma et al. 2008), while the existence of such cool electrons is well studied for supernova remnants and solar winds (van Adelsberg et al. 2008; Vink et al. 2015). As shown in Figure 1, a clear method for identifying non-energized electrons in GRB afterglows is the measurement of their Faraday effect that suppresses the radio polarization but keeps the higher frequency (e.g. optical) one as emitted (Toma et al. 2008). **The intensive studies of non-energized electrons in a number of afterglows will make a revolutionary change in the GRB progenitors, because diversity of GRB afterglows are likely linking with types of progenitor stars.**

Quite limited theoretical works investigated the fraction of non-energized electrons in GRB studies. One of the critical reasons was the absence of a suitable method to constrain the fraction before the ALMA era. Hence, most related theoretical models simply assume that all the electrons are energized by the ultra-relativistic shock and emit the observed afterglow (100% energized case). The measurement of $E_{tot} = E_\gamma + E_{AG}$ of $\sim 10^{51}$ erg has been estimated for several events, and the standard mass of progenitor star $\sim 30M_\odot$ is preferred for classical long GRBs. Here, E_γ and E_{AG} are radiated energies in prompt and afterglow phases as synchrotron radi-

ations, respectively. However, a substantial fraction of the electrons likely remain cool at the moment of the shock and do not emit observable radiation (i.e., high synchrotron absorption)(Toma et al. 2008). In this case, however, the energy related to this non-energized electron component, hidden energy $E_{AG,h}$, increases the required total energy, which is, $E_{tot} = E_\gamma + E_{AG} + E_{AG,h}$. Theoretically, the revised E_{tot} could be larger than 10^{52} erg (Mészáros & Rees 2010; Toma et al. 2011). In this extreme but quite expectable case, the standard scenario of the $\sim 30M_\odot$ progenitor would be inapplicable; however, extremely massive stars (e.g. $\sim 300M_\odot$) would be required to be progenitors of such GRBs. Therefore, observationally identifying of the non-energized electron component is essential and a unique approach to constraining the mass of GRB progenitors.

Urata et al. (2019) demonstrated the first linear polarization detection on GRB171205A and the weak detection implied the existence of non-energized cool electrons assuming optical linear polarization of 1% (the purple box of Figure 1). Following the successful measurement, two more polarimetry have been executed with coordinated optical polarimetry for precise measurements of non-energized electrons.

ngVLA can enhance this study for applying this new method for various types of GRBs. The high sensitivity of ngVLA can apply the method for most of all types of GRBs including short GRB afterglows that are hardly characterized using current instruments. Multi-frequency polarimetry at the same day with ngVLA also can provide accurate measurements of the fraction of non-energized cool electrons by characterizing the polarization spectrum (Figure 1).

4. Characterization of High-z GRBs

GRBs are currently being exploited as probes of the early Universe. Afterglow observational studies have revealed that

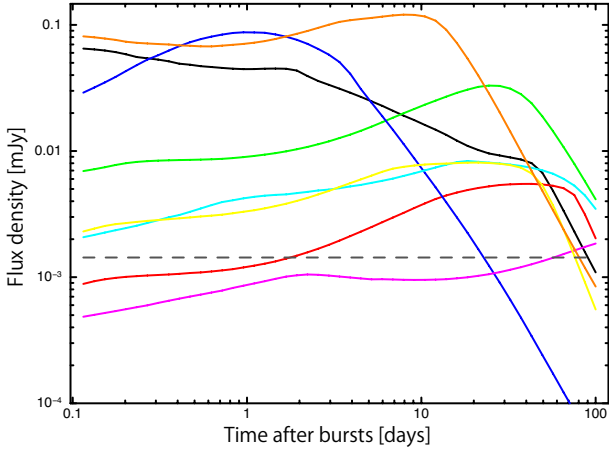


Fig. 3. Expected afterglow light curves at $z = 12$. The dashed line indicates the 5σ sensitivity of ngVLA. The black line indicates the model function based on the numerical modeling for high- z ($z = 8.3$) GRB090423 (Figure 5).

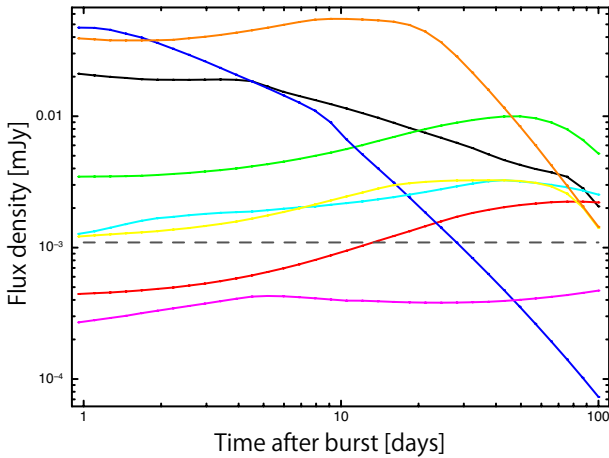


Fig. 4. Expected afterglow light curves at $z = 30$. The dashed line indicates the 5σ sensitivity of ngVLA. The black line indicates the model function based on the numerical modeling for high- z ($z = 8.3$) GRB090423 (Figure 5).

the majority of long GRBs occur as a result of the death of massive stars (e.g., Stanek et al. 2003). Since the highest- z events at the reionization epoch ($z \sim 9$) have already been observed (Tanvir et al. 2009), and their discovery at $z > 10$ is highly possible (e.g., Bloom et al. 2009), long GRBs are unique and powerful means to study explosions of first-generation stars and to explore reionization and dusts creation history by GRB as light source (e.g., Totani et al. 2006; Perley et al. 2010; Jang et al. 2011). Hence, understanding of the physical properties of long GRBs could probe the physical conditions of early Universe and first-generation stars.

The brightness of GRB afterglows are generally brighter than other possible explosions from the first generation stars such as pair-instability supernova. Figure 3 shows the expected afterglow light curves at $z = 12$ in the 16 GHz band based on physical parameters obtained by numerical forward shock modelings for high- z (e.g., Figure 5) and lower- z GRB after-

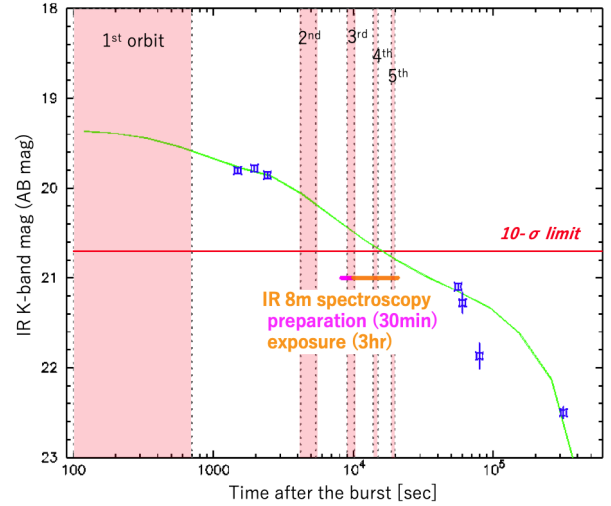


Fig. 5. IR K-band light curve of GRB090423 ($z = 8.3$) with external synchrotron model. The green line indicates the best fitted model based on external forward shock synchrotron radiation. The corresponding model lines for this event are also shown in Figure 3 & 4 with the black lines. The red boxes indicate the observing window using autonomous IR follow-ups by future satellite missions such as HiZ-GUNDAM and THESEUS.

glows (e.g., Table 1). As described in §2, these light curve and SED monitoring will provide explosion physical parameters. Thanks to high sensitivity of ngVLA, the fraction of non-energized cool electrons are also possible (described in §3). These physical parameters and total energetic measurements therefore enable to reveal the properties of first generation stars.

The high signal-to-noise ratio (S/N) observations may be able to search for atomic and molecular absorption lines and then enable to estimate redshift for these high- z GRBs (Inoue et al. 2007). Current redshift estimation of GRBs is relied on Ly α break, metal absorption lines in afterglows spectrum and emissions lines from host galaxies through OIR spectroscopy. Since OIR afterglow is generally faded out rapidly, timely OIR spectroscopy is required (e.g. Figure 5). These observations are sometimes affected by weather and available instruments on large OIR telescopes. The lifetime of radio afterglows in the ngVLA band is usually long (Figure 3) and high sensitivity ngVLA observations would be able to measure redshifts once the atomic and molecular absorption method is established. The accurate position determined by ngVLA for high- z GRBs also enable to perform deep IR searches for their host galaxies using JWST and future large missions (e.g. LUVOIR). The host galaxies study at high- z using ngVLA may not be appropriate, because the long life time of radio afterglows.

In 2020th/2030th, two satellite missions, HiZ-GUNDAM (Yonetoku et al. 2020) and THESEUS (Amati et al. 2018) are planned and will be able to provide GRB alerting up to $z \sim 12 - 14$ with reasonable position accuracies (i.e. arc-sec level with IR counterparts or several arcmin without IR counterparts). These missions will select high- z GRBs based on OIR photometric redshift method. In this case, these missions may not be able to provide timely GRB alerts for OIR spectroscopy on very high- z events (e.g., only single detec-

tion in the red band). Although OIR follow-up may not be able to determine their redshifts, the coordination with ngVLA follow-ups would provide new approaches. By responding to these high- z GRB position alerts, ngVLA can detect the majority of GRB afterglows (Figure 3). In addition to these satellite missions, the planned Large Submillimeter Telescope (LST; Kawabe et al. 2016) would provide high- z GRBs up to $z \sim 30$ by the high cadence radio time-domain surveys for radio flashes originated from GRB reverse shock. The associated afterglow from forward shock can be also observed by ngVLA (Figure 4).

5. GRB/SN-SNR connection

The long GRBs are originated from massive stellar explosions. This confirmation was made by the optical spectroscopy in the afterglow phase (~ 10 days-several week) by identifying SNe component resemble to the type Ic supernova and feature broad lines implying fast moving ejecta with velocities $\sim 0.1c$ (Mazzali et al. 2007; Hjorth & Bloom 2012). If there is an associated SNe, jets are not the only ejecta expelled in the GRB events, a spherical outflow is also present. After the explosion, the SN ejecta will remain in free expansion for a few decades, and will sweep up material from the surrounding medium. The SN ejecta interacts with the surrounding medium, accelerating particles to relativistic speeds and amplifying the magnetic field, producing radio synchrotron emission much like in a typical SN remnant.

The radio emission peaks when SNe has swept up an equivalent mass to the initial ejected mass, at the Sedov-Taylor time. Due to the explosion velocity measured by optical spectrum is large, the Sedov-Taylor time of GRB is expected to be 2 orders of magnitude shorter than typical supernova remnant (Barniol Duran & Giannios 2015). The expected time scale is 10~several 10 years, although it also depends on several parameters as same as radiation from GRB jets. With this shorter timescale than typical SNR, observations of SNR associated with GRB could be managed for ~ 10 GRB samples at $z < 0.2$ (Barniol Duran & Giannios 2015). Detecting the radio rebrightening of long GRB caused by the associated SN transform into an SNR would enrich the understanding of the stellar explosion.

Several efforts have been made for finding the radio radiations. VLA observed three nearby SNe associated GRB and constrained on the density of the surrounding medium for various assumed values of the microphysical parameters related to the magnetic field and synchrotron-emitting electrons (Peters et al. 2019). The ALMA observations targeted on host galaxies (around ~ 10 years after the GRB) detected an unexpected radio variability which is not explained by the external synchrotron shock radiation. Since the early phase of X-ray and optical afterglows can be explained by the external synchrotron shock model, the radio variability may be related with SNe and/or SNR radiations (Huang et al. 2021 in prep.). These observations are suffering from the sensitivity limitation of the current instruments. Further detailed observations with high sensitivity are therefore required. ngVLA has two advantages; (i) characterization of their radiation and measuring physical parameters by high sensitivity flux measurements and (ii) di-

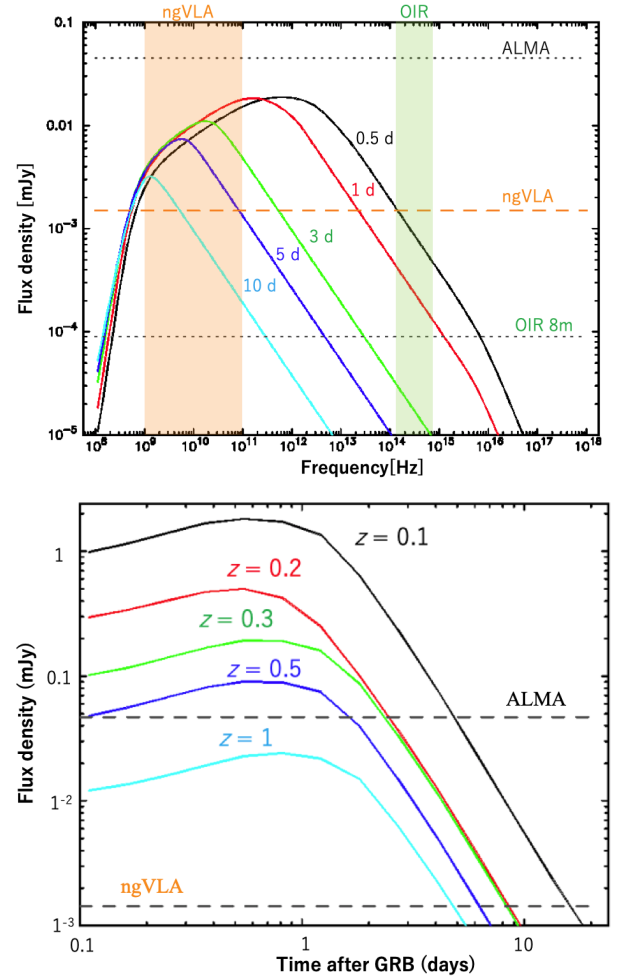


Fig. 6. Top: Expected SED temporal evolution of short GRB afterglow at $z = 1$. Bottom: Expected light curves of short GRBs at various redshifts. The redshift range of currently observed short GRBs are 0~2.5. ngVLA can characterize majority of short GRBs.

rect imaging of the expansion with high sensitivity and angular resolution capabilities.

6. Short GRBs

Short GRBs are sudden flashes of γ -rays with durations shorter than 2 seconds. Their γ -ray properties as well as their environments (e.g., ambient density and location in their host galaxies) are consistent with the popular scenario of neutron star (NS) mergers. The first GW event from a NS merger, GW 170817, was observed by LIGO and Virgo and associated with the short GRB (Abbott et al. 2017). A bright kilonova emission was also discovered in UV, optical and near-IR bands. Furthermore, the X-ray afterglow started to rise several days after the GW trigger revealing the presence of a relativistic jet viewed off-axis. These rich results are basically described by the off-axis short GRB model with r-process elements synthesized in the ejecta (e.g., Alexander et al. 2017; Haggard et al. 2017; Lazzati et al. 2017; Murguía-Berthier et al. 2017; Ioka & Nakamura 2018; Jin et al. 2018; Kathirgamaraju et al. 2018; Troja et al. 2018; Troja et al. 2019). However, the as-

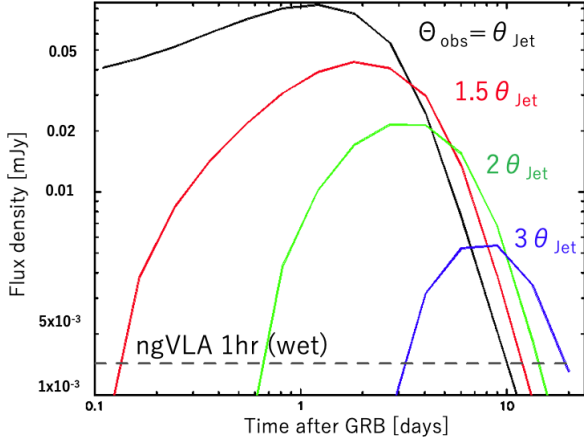


Fig. 7. Expected short GRB afterglow light curves at $z = 0.3$ in the 100 GHz band along with jet viewing angles.

sociation of short GRBs and GWs is still unclear due to the atypical properties of GRB 170817A. After the discovery of GW 170817/GRB 170817A, understanding the nature of short GRBs, in general, becomes incredibly important. Estimations of explosion parameters of on-axis short GRB are therefore critical as the solid on-axis template for understanding of the off-axis origin of GRB170817A. The broader community also pays attention to these estimations, because of the connection between short GRBs and GW transients.

As VLA, SMA and ALMA demonstrated multi-frequency observations for long-GRBs, the radio observations have been playing a key role in deriving burst explosion physical parameters by characterizing of the synchrotron radiation (e.g., van Eerten et al. 2012; Urata et al. 2014; Urata et al. 2015a; Huang et al. 2017). Using the same method, the unified picture of the off-axis jet model for long GRBs was verified by examining the properties of X-ray Flash (XRFs; Urata et al. 2015b). Unlike long GRBs, short GRB afterglows tend to faint possibly due to low circumburst density or smaller explosion energy. These properties make short GRB afterglows fainter than those of long GRBs and the observations of short GRB afterglows require higher sensitivities and much rapid response in the higher frequency side. Figure 6 is the expected spectrum temporal evolution at $z = 1$ and light curves at various redshift using lower circumburst density and smaller explosion energy (other micro physical parameters are identical to those of long GRBs shown in Figure 2 left). Thanks to high sensitivity of ngVLA, short GRB afterglows even at higher redshift (e.g., $z = 1$) could be observed (Figure 6). Since the currently observed redshift range of short GRBs is $0 < z < 2.5$ (average of $z \sim 0.5$), ngVLA could provide concrete on-axis template for understanding of off-axis short GRBs by observing majority of short events.

ngVLA would also be able to characterize off-axis events Figure 7 shows expected short GRB afterglows along with viewing angles (i.e., off-axis short GRB orphan afterglows). Since off-axis short GRBs in their prompt phase become softer spectrum and fainter apparent luminosity, position alerts from GRB satellites may not be available for these off-axis events.

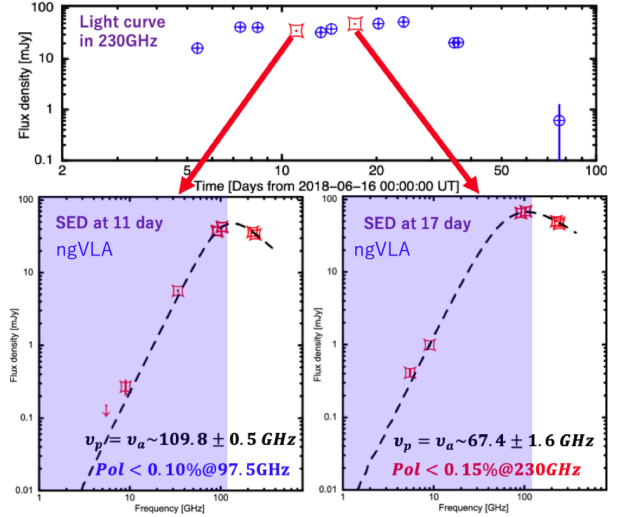


Fig. 8. One of examples of unique stellar transient, AT2018cow as the candidate of EM counterpart of neutrino. The radiation is characterized by synchrotron radiation. As identical to the GRB external synchrotron model, the peak frequency shifts to lower frequency side along with time. Radio polarimetry is also the critical tool for revealing their nature (Huang et al. 2019).

In this case, coordinated observations with wide field time domain surveys in OIR (e.g., LSST) and radio (e.g., SKA) are required.

7. Transients as high energy cosmic-rays and neutrino sources

The origin of the highest-energy cosmic rays is believed to be extragalactic, but their acceleration sites remain unidentified. High-energy neutrinos are expected to be produced in or near the acceleration sites when cosmic rays interact with matter and ambient light, producing charged mesons that decay into neutrinos and other particles. Unlike cosmic rays, neutrinos can travel through the Universe unimpeded by interactions with other particles and undeflected by magnetic fields, providing a means to identify and study the extreme environments producing cosmic rays. The first EM counterpart of high energy neutrinos was identified as blazar (IceCube Collaboration et al. 2018b; IceCube Collaboration et al. 2018c). The measurement has a major impact on our view of the non-thermal universe, but understanding cosmic accelerators require a substantial increase in the number of multi-messenger observations.

As IceCube and the multi-messenger community demonstrated, high-energy γ -ray observations using Fermi/LAT were key to identifying the counterpart (IceCube Collaboration et al. 2018c). Although more than 60 neutrino events were followed-up by the same method using Fermi after the 1st EM counterpart discovery in 2017, none of them were identified as the 2nd neutrino counterpart. This indicates that the origin of the events is not only blazar and the search method using Fermi/LAT are inadequate. Other possible EM counterparts of high-energy neutrinos are proposed to be tidal disruption flares (TDE; Wang et al. 2011; Wang & Liu 2016; Senno et

al. 2017; Dai & Fang 2017; Lunardini & Winter 2017) and GRBs (Murase & Ioka 2013) that also share similar ultra-relativistic jets. In addition to these transients, Huang et al. (2019) also demonstrated with the ALMA polarimetry that the new type of optical transient (i.e. fast-rising blue optical transient, AT2018cow type of stellar explosion) is possible counterpart. In fact, IceCube also reported the possible neutrinos detection from AT2018cow (IceCube Collaboration et al. 2018a). All of these transients have the mm/submm counterparts in various time scales and characterizing their synchrotron radiation would provide explosion parameters by identifying the synchrotron peak frequency and the peak spectral flux density (e.g., Zauderer et al. 2011; Huang et al. 2019). Figure 8 shows one of the examples of radio flux and polarimetric monitoring on AT2018cow. These observations revealed that new types of transients discovered by the synoptic optical transient survey is a unique stellar explosion and possible PeV cosmic-ray accelerator (Huang et al. 2019). The high sensitivity ngVLA photometric and polarimetric monitoring can therefore reveal the nature of various transients and promote multi-messenger astronomy.

8. Synergy with other future missions

8.1. GRB satellite missions

There is no doubt that dedicated transient satellite missions with multi-frequency capability are required for promoting further GRB cosmology and multi-message astrophysics as the *Swift* mission demonstrated. In 2020th and 2030th, HiZ-GUNDAM (Yonetoku et al. 2020) and THESEUS (Amati et al. 2018) are planned by JAXA and ESA, respectively. Their autonomic IR observations from soon after explosions are key to use GRBs as probe of the early universe. Localization of short GRBs (arcmin level) and its high-sensitivity IR (equivalent to ground-based 4-m class telescope) monitoring are also essential to characterize GW transients and associated kilo/macronova radiation caused by NS-NS or NS-BH mergers. Hence, coordinations with these missions are key to promote sciences described in §4 and §6.

These GRB missions will also provide other high energy transients. One of the critical findings by the hard X-ray survey of *Swift* was the first TDE (Burrows et al. 2011). Followed by the discovery, numbers of TDE have been identified by optical wide field surveys (e.g., Gezari et al. 2012). ngVLA follow-ups will characterize their non-thermal radiation and promote multi-messenger astronomy (§7).

8.2. Optical Transient Surveys

Time-domain surveys in various wavelengths have been making mysterious new transients discoveries. These results are remarkable, and newly discovered transients are revolutionizing our knowledge of astronomy and astrophysics. Optical untargeted imaging surveys such as CRTS, PTF, Pan-STARRS-1, ZTF (Drake et al. 2009; Law et al. 2009; Chambers et al. 2016; Bellm et al. 2019). have also been discovering new stellar explosions such as super-luminous super nova (SLSNe), energetic SNe, and fast-rising blue optical transient (i.e. FBOT such as AT2018cow in §7). Since SLSNe and energetic SNe are suggested to have the common powerful central energy

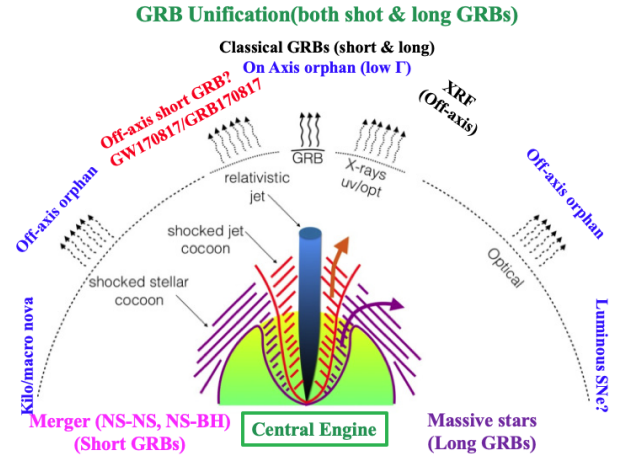


Fig. 9. Unification picture of GRBs along with jet viewing angle and Lorentz factor (or power). The background figure is from Nakar, & Piran 2017.

source to that of GRBs (e.g., Pastorello et al. 2010; Kann et al. 2019; Izzo et al. 2020), the unification picture of massive stellar transient along with GRB jet viewing angle (identical to that of AGN; Figure 9) may be studied by the direct imaging of GRB-SNR (§5). As described in §7, the AT2018cow type new transient is one of potential neutrino counterparts. In the era of ngVLA, numbers of optical time domain surveys using smaller telescopes may be available. As AT2018cow was discovered by the ATLAS 0.5 m telescope, these optical surveys would be very powerful to promote science cases described in §5 & §7.

A coordination with radio transient surveys such as SKA and LST may be able to make further understanding of off-axis short GRB afterglow (i.e. orphan GRBs) related with GW counterparts (§6). Although ngVLA can characterize the properties of off-axis short GRB afterglows (Figure 7), the finding of events must be performed by other instruments (e.g., Lamb et al. 2018; Huang et al. 2020). Since GRB satellite missions are inadequate for finding off-axis short GRBs, the wide field time domain surveys in OIR (e.g. LSST) and radio (e.g. SKA, LST) are required. Especially, radio survey may be efficient for finding of off-axis short GRB orphan afterglows because of sensitivities of instruments, life time of afterglows, and classification of transients.

This work is supported by the Ministry of Science and Technology of Taiwan grants MOST 105-2112-M-008-013-MY3 (Y.U.).

References

- Abbott, B. P., Abbott, R., Abbott, T. D., et al. 2017, *ApJL*, 848, L13. doi:10.3847/2041-8213/aa920c
- Alexander, K. D., Berger, E., Fong, W., et al. 2017, *ApJL*, 848, L21
- Amati, L., O’Brien, P., Götz, D., et al. 2018, *Advances in Space Research*, 62, 191. doi:10.1016/j.asr.2018.03.010
- Barniol Duran, R. & Giannios, D. 2015, *MNRAS*, 454, 1711. doi:10.1093/mnras/stv2004
- Bellm, E. C., Kulkarni, S. R., Graham, M. J., et al. 2019, *PASP*, 131,

018002. doi:10.1088/1538-3873/aaecbe
- Bloom, J. S., Perley, D. A., Li, W., et al. 2009, *ApJ*, 691, 723. doi:10.1088/0004-637X/691/1/723
- Burrows, D. N., Kennea, J. A., Ghisellini, G., et al. 2011, *Nature*, 476, 421. doi:10.1038/nature10374
- Cenko, S. B., Kulkarni, S. R., Horesh, A., et al. 2013, *ApJ*, 769, 130
- Chambers, K. C., Magnier, E. A., Metcalfe, N., et al. 2016, arXiv:1612.05560
- Dai, L. & Fang, K. 2017, *MNRAS*, 469, 1354. doi:10.1093/mnras/stx863
- Drake, A. J., Djorgovski, S. G., Mahabal, A., et al. 2009, *ApJ*, 696, 870. doi:10.1088/0004-637X/696/1/870
- Gezari, S., Chornock, R., Rest, A., et al. 2012, *Nature*, 485, 217. doi:10.1038/nature10990
- Godet, O., Paul, J., Wei, J. Y., et al. 2012, *Proc. SPIE*, 8443, 84431O. doi:10.1117/12.925171
- Haggard, D., Nynka, M., Ruan, J. J., et al. 2017, *ApJL*, 848, L25
- Huang, K., Urata, Y., Takahashi, S., et al. 2017, *PASJ*, 69, 20
- Huang, K., Shimoda, J., Urata, Y., et al. 2019, *ApJL*, 878, L25. doi:10.3847/2041-8213/ab23fd
- Huang, Y.-J., Urata, Y., Huang, K., et al. 2020, *ApJ*, 897, 69. doi:10.3847/1538-4357/ab8f9a
- Blaufuss, E. 2018, *The Astronomer's Telegram*, 11785
- IceCube Collaboration, Aartsen, M. G., Ackermann, M., et al. 2018, *Science*, 361, 147. doi:10.1126/science.aat2890
- IceCube Collaboration, Aartsen, M. G., Ackermann, M., et al. 2018, *Science*, 361, eaat1378. doi:10.1126/science.aat1378
- Inoue, S., Omukai, K., & Ciardi, B. 2007, *MNRAS*, 380, 1715. doi:10.1111/j.1365-2966.2007.12234.x
- Ioka, K., & Nakamura, T. 2018, *Progress of Theoretical and Experimental Physics*, 2018, 043E02
- Izzo, L., Auchettl, K., Hjorth, J., et al. 2020, *A&A*, 639, L11. doi:10.1051/0004-6361/202038152
- Jang, M., Im, M., Lee, I., et al. 2011, *ApJL*, 741, L20. doi:10.1088/2041-8205/741/1/L20
- Jin, Z.-P., Li, X., Wang, H., et al. 2018, *ApJ*, 857, 128
- Hjorth, J. & Bloom, J. S. 2012, Chapter 9 in "Gamma-Ray Bursts, 169
- Kann, D. A., Schady, P., Olivares E., F., et al. 2019, *A&A*, 624, A143. doi:10.1051/0004-6361/201629162
- Kathirgamaraju, A., Barniol Duran, R., & Giannios, D. 2018, *MNRAS*, 473, L121
- Kawabe, R., Kohno, K., Tamura, Y., et al. 2016, *Proc. SPIE*, 9906, 990626. doi:10.1117/12.2232202
- Lamb, G. P., Tanaka, M., & Kobayashi, S. 2018, *MNRAS*, 476, 4435. doi:10.1093/mnras/sty484
- Law, N. M., Kulkarni, S. R., Dekany, R. G., et al. 2009, *PASP*, 121, 1395. doi:10.1086/648598
- Lazzati, D., López-Cámara, D., Cantiello, M., et al. 2017, *ApJL*, 848, L6
- Lunardini, C. & Winter, W. 2017, *Phys. Rev. D*, 95, 123001. doi:10.1103/PhysRevD.95.123001
- Mazzali, P. A., Kawabata, K. S., Maeda, K., et al. 2007, *ApJ*, 670, 592. doi:10.1086/521873
- Mészáros, P. & Rees, M. J. 1997, *ApJ*, 476, 232. doi:10.1086/303625
- Mészáros, P. & Rees, M. J. 2010, *ApJ*, 715, 967. doi:10.1088/0004-637X/715/2/967
- Murase, K. & Ioka, K. 2013, *Phys. Rev. Lett.*, 111, 121102. doi:10.1103/PhysRevLett.111.121102
- Murguía-Berthier, A., Ramirez-Ruiz, E., Kilpatrick, C. D., et al. 2017, *ApJL*, 848, L34
- Nakar, E., & Piran, T. 2017, *ApJ*, 834, 28
- Pastorello, A., Smartt, S. J., Botticella, M. T., et al. 2010, *ApJL*, 724, L16. doi:10.1088/2041-8205/724/1/L16
- Perley, D. A., Bloom, J. S., Klein, C. R., et al. 2010, *MNRAS*, 406, 2473. doi:10.1111/j.1365-2966.2010.16772.x
- Peters, C., van der Horst, A. J., Chomiuk, L., et al. 2019, *ApJ*, 872, 28. doi:10.3847/1538-4357/aafb3c
- Sari, R., Piran, T., & Narayan, R. 1998, *ApJL*, 497, L17. doi:10.1086/311269
- Senno, N., Murase, K., & Mészáros, P. 2017, *ApJ*, 838, 3. doi:10.3847/1538-4357/aa6344
- Stanek, K. Z., Matheson, T., Garnavich, P. M., et al. 2003, *ApJL*, 591, L17. doi:10.1086/376976
- Tanvir, N. R., Fox, D. B., Levan, A. J., et al. 2009, *Nature*, 461, 1254. doi:10.1038/nature08459
- Toma, K., Ioka, K., & Nakamura, T. 2008, *ApJL*, 673, L123
- Toma, K., Sakamoto, T., & Mészáros, P. 2011, *ApJ*, 731, 127. doi:10.1088/0004-637X/731/2/127
- Totani, T., Kawai, N., Kosugi, G., et al. 2006, *PASJ*, 58, 485. doi:10.1093/pasj/58.3.485
- Troja, E., Piro, L., Ryan, G., et al. 2018, *MNRAS*, 478, L18
- Troja, E., van Eerten, H., Ryan, G., et al. 2019, *MNRAS*, 489, 1919
- Urata, Y., Huang, K., Takahashi, S., et al. 2014, *ApJ*, 789, 146
- Urata, Y., Huang, K., Asada, K., et al. 2015, *Advances in Astronomy*, 2015, 165030
- Urata, Y., Huang, K., Yamazaki, R., & Sakamoto, T. 2015, *ApJ*, 806, 222
- Urata, Y., Toma, K., Huang, K., et al. 2019, *ApJL*, 884, L58
- van Adelsberg, M., Heng, K., McCray, R., & Raymond, J. C. 2008, *ApJ*, 689, 1089
- van Eerten, H., van der Horst, A., & MacFadyen, A. 2012, *ApJ*, 749, 44
- Vink, J., Broersen, S., Bykov, A., & Gabici, S. 2015, *A&A*, 579, A13
- Wang, X.-Y., Liu, R.-Y., Dai, Z.-G., et al. 2011, *Phys. Rev. D*, 84, 081301. doi:10.1103/PhysRevD.84.081301
- Wang, X.-Y. & Liu, R.-Y. 2016, *Phys. Rev. D*, 93, 083005. doi:10.1103/PhysRevD.93.083005
- Yonetoku, D., Mihara, T., Doi, A., et al. 2020, *Proc. SPIE*, 11444, 114442Z
- Zauderer, B. A., Berger, E., Soderberg, A. M., et al. 2011, *Nature*, 476, 425. doi:10.1038/nature10366